IA-1357

ELECTRON PARAMAGNETIC RESONANCE STUDIES OF DEFECTS IN DILUTE MAGNETIC ALLOYS

J.T. Suss and A. Raizman

Israel Atomic Energy Commission
Soreq Nuclear Research Centre

This publication may be obtained at the following address:
Library and Technical Information Dept.
Soreq Nuclear Research Centre
Yavne 70600, ISRAEL

ניתן להשיג את הפרסום הזה
על ידי פנייה לכתובת:
מחלקת תיעוד וספריה
המרכז למחקר גרעיני
נחל שורק דואר יבנה 70600, ישראל

IA-1357

Israel Atomic Energy Commission

SUSS, J.T and RAIZMAN, A.

Electron paramagnetic resonance studies of defects in dilute magnetic alloys

Jan. 1980 68 p. 14 figs. 3 tables

The EPR spectrum of erbium was used to study the effects of cold-working (rolling and mechanical polishing) in dilute gold-erbium alloys.

./..

IA-1357

Israel Atomic Energy Commission

SUSS, J.T. and RAIZMAN, A.

Electron paramagnetic resonance studies of defects in dilute magnetic alloys

Jan. 1980 68 p. 14 figs. 3 tables

The EPR spectrum of erbium was used to study the effects of cold-working (rolling and mechanical polishing) in dilute gold-erbium alloys.

./..

IA-1357

Israel Atomic Energy Commission

SUSS, J.T. and RAIZMAN, A.

Electron paramagnetic resonance studies of defects in dilute magnetic alloys

Jan. 1980 68 p. 14 figs. 3 tables

The EPR spectrum of erbium was used to study the effects of cold-working (rolling and mechanical polishing) in dilute gold-erbium alloys.

./..

Variation in the EPR linewidth, intensity and asymmetry parameter (A/B ratio) were investigated. Most of the results could be interpreted in terms of segregation of erbium ions to subgrain boundaries (dislocations) in a surface layer of a few thousand Angstroms.

Variation in the EPR linewidth, intensity and asymmetry parameter (A/B ratio) were investigated. Most of the results could be interpreted in terms of segregation of erbium ions to subgrain boundaries (dislocations) in a surface layer of a few thousand Angstroms.

Variation in the EPR linewidth, intensity and asymmetry parameter (A/B ratio) were investigated. Most of the results could be interpreted in terms of segregation of erbium ions to subgrain boundaries (dislocations) in a surface layer of a few thousand Angstroms.

IA - 1357

ELECTRON PARAMAGNETIC RESONANCE STUDIES OF DEFECTS IN DILUTE MAGNETIC ALLOYS

J.T. Suss and A. Raizman

Israel Atomic Energy Commission
January 1980

This report was submitted in Feb. 1979 to the US-Israel Binational Science Foundation (BSF), Jerusalem, Israel as the final report on project No. 777.

CONTENTS

L I S T O F F I G U R E S

Fig. 11. Computer fitted and measured EPR spectrum of a heated sample of Au doped with 1500 ppm Er, over a range of 1000 Gauss.

Fig. 12. The A/B ratio as a function of the amount of absorption and dispersion calculated for a Lorentzian line.

Fig. 13. Calculated variations in the A/B ratio due to the hyperfine structure, as a function of the linewidth for the case of Er with a Lorentzian lineshape.

Fig. 14. Skin depth δ (at 9.4 GHz) and residual resistivity ρ in Au doped with Er as a function of the concentration of Er.

LIST OF ABBREVIATIONS

A	maximum of the first derivative of the EPR absorption line
$\overset{o}{A}$	Angstrom
a	residual linewidth
a_r	residual linewidth in rolled samples
a_h	residual linewidth in heated samples
B	maximum of the first derivative of the EPR absorption line
b	Korringa relaxation rate
A/B	asymmetry parameter of the first derivative of the EPR absorption line
BSF	Binational Science Foundation
C	degrees Centrigrade
c	impurity concentration
c_o	velocity of light
D	diffusion coefficient
δ	skin depth
EPR	electron paramagnetic resonance
G	gauss
g	g-factor
g_d	localized spin g-factor
g_s	conduction electron g-factor
H	magnetic field
H_o	field of resonance
ΔH	EPR linewidth

DH_o	residual linewidth due to random stress
DH_c	Er concentration dependent contribution to residual linewidth
DH_k	Korringa contribution to the linewidth
h_o	thickness of sample before rolling
h_i	thickness of sample after i-th rolling step
Δh	decrease in the thickness of sample after i-th rolling step, with respect to h_o.
I	intensity of the EPR line
I_o	multiplication factor for computer fitting
η	electron density of states at Fermi surface
J	exchange parameter
K	degrees Kelvin
$\vec{k}$	wave vector
k_B	Boltzmann's constant
k_F	wave number at the Fermi surface
χ'	real part of magnetic susceptibility
χ''	imaginary part of magnetic susceptibility
χ_d	susceptibility of the localized spins
χ_s	susceptibility of the conduction electrons
λ	molecular field constant
λ_o	wavelength
M	magnetization
N	number of spins
N'	number of atoms per unit cell
μ_o	permeability in vacuum

μ_B	Bohr magneton
μ_r	relative permeability of conductor
ppm	parts per milion
ρ	electrical resistivity
σ	electrical conductivity
τ	collision time
T	temperature
T_2	electron spin relaxation time
T_D	time it takes the magnetization to diffuse through the skin depth δ
T_{dd}	relaxation time describing the concentration dependent part of the linewidth
T_{dl}	impurity-spin lattice relaxation time
T_{sl}	electron-spin lattice relaxation time
TE	transverse electric mode in microwave cavity
U(q)	electron-electron Coulomb interaction
V	volume of unit cell
V_F	electron velocity at the Fermi surface

ELECTRON PARAMAGNETIC RESONANCE STUDIES OF DEFECTS IN DILUTE MAGNETIC ALLOYS

J.T. Suss and A. Raizman

ABSTRACT

An electron paramagnetic resonance (EPR) study of the effects of cold-working (rolling and mechanical polishing) and ion bombardment (by argon and gold ions) on the EPR spectrum of Er in Au is reported. Pellets of dilute alloys of Au doped with Er were prepared in an arc furnace. From the pellets, samples in the form of thin foils and plates were made by rolling at room temperature. The resonance experiments were performed at X-band and at temperatures between 1.65 and 4.2 K. Heating of the rolled samples reduced the EPR linewidth and intensity, and increased the value of the asymmetry parameter (the A/B) ratio). Ion bombardment produced partial recovery, gradual deformation by successive rolling yielded almost complete recovery and mechanical polishing resulted in complete recovery of the linewidth, intensity and A/B ratio to values observed before heating. No appreciable variations were detected in the g-factor, hyperfine structure constant or the Korringa relaxation rate. The extremely narrow absorption line of Er obtained after the heat treatment is narrower than any other value previously reported for a magnetic impurity in polycrystalline metals at X-band, and thus makes it a more sensitive probe for the study of defects in metals and alloys. Most of our results can be explained in terms of segregation of erbium ions to subgrain boundaries (dislocations) in a surface layer of a few thousand Å. A theoretical treatment is presented for the behavior of the linewidth. Theoretical estimates for the upper and lower limits of the number of Er ions contributing to the absorption line after the heat treatment are found to be in good agreement with the experimental results. Our results also show that Er produces much less local stress in Au than in Ag. The EPR of magnetic impurities in metals appears to be a promising technique for the study of interactions between magnetic impurities and defects produced in metals by cold-working and irradiation.

I. INTRODUCTION

The original objective of the present research was to determine to what extent the electron paramagnetic resonance (EPR) technique can be used to investigate irradiation effects in dilute magnetic alloys. In the majority of the studies of radiation damage in metals and alloys the bulk properties of the metals were investigated, using methods such as resistivity measurements, susceptibility, measurement of various mechanical properties of the metals, etc.[1]. All these methods yielded information on the macroscopic properties of the damage.

EPR has been found a powerful tool for the investigation of the electronic properties of magnetic impurities in metals, of interactions between conduction electrons and magnetic impurities, and of the interactions between the magnetic impurities themselves[2]. Therefore the EPR technique seemed a very promising tool for the study of the microscopic properties of radiation damage in metals.

During the course of this study an unforeseen difficulty arose, the electron accelerator at the Hebrew University which was intended to be the main irradiation source for this research suddenly became unavailable to us and we had to turn to another suitable radiation source for our experiments[3]. Ion bombardment was found to be a suitable as well as an available irradiation source. Permission was obtained to carry out the irradiations at the ion implantation laboratory at the Technion. In parallel we also decided to follow

up a new and promising avenue of research: the study of defects produced in metals by cold-work. The BSF was advised accordingly[3].

By studying the behavior of the EPR spectrum of Er in Au, in cold-worked (rolled and polished), heat treated and ion bombarded (with argon and gold ions) samples we were able to show that EPR is a powerful technique for the study of the behavior of the defects and for the study of the interactions between the defects and the magnetic impurities in dilute gold-erbium alloys. The extension of this work to other metal - magnetic impurity systems is obvious.

II. EXPERIMENTAL TECHNIQUES

Sample preparation and treatments: The alloys used in this study were prepared by melting 99.999% pure Au (supplied by Leico Industries Inc., N.Y., USA) with Er added as an impurity. To achieve high accuracy in the doping levels, first an alloy of $Au_{98.4\%}Er_{1.6\%}$ was prepared, which was further diluted to the required doping levels of Er. An arc furnace with a water-cooled copper hearth was used to prepare the alloys. The samples obtained were in the form of small pellets, with nominal concentrations of 100, 300, 600, 1000, 1500 and 2000 ppm of Er. The pellets were cleaned by etching in aqua regia and washed in distilled water. After cleaning, they were rolled at room temperature into plates and foils. Most experiments were performed with foils 0.1mm thick. The samples were passed through a manually operated roller at an average speed of approximately 2cm/sec. To prevent contamination of the samples with iron from the rollers, the rolling was performed between 0.1mm thick tantalum sheets. Samples

were cut from the foils into a size usually 8x12mm suitable for mounting in the cavity of the EPR spectrometer.

Thermal treatment of the samples consisted of heating in a quartz tube for 1 hour at 400C (half the absolute melting temperature of Au) in either (a) a dynamic vacuum of 10^{-6} torr followed by slow cooling (cooling times between 1 and 3 minutes), or (b) hydrogen followed by slow cooling, or (c) an argon atmosphere followed by quenching to 0C; quenching time was approximately 1 second, or (d) air followed by slow cooling. Some heat treatments at 400C in air were also done for 4 and 8 hours.

The EPR spectrometer: A VARIAN Type EC-365 X-band EPR spectrometer with a standard liquid helium dewar and an immersed rectangular TE_{012} cavity was used. The samples (in the form of thin foils) were pasted on the narrow side of the cavity. In the series of measurements always the same face of the foil (i.e. the side not pasted to the cavity wall) was exposed to the microwave radio frequency field.

Computer: An IBM 370/165 computer at the Weizmann Institute, through the Soreq PDP 1134A computer terminal, was used for lineshape calculations and fittings.

Ion implantation: The ion implantation was performed at the Technion, Israel Institute of Technology, ion implantation laboratory, headed by Prof. R. Kalisch. Our samples were bombarded with argon ions, which were implanted with energies up to 340keV and with doses up to $2.5x10^{16}$ ions/cm^2. Gold ions were implanted with energies up to

340 keV, and a dose of 2×10^{16} ions/cm^2. The ion implantation was carried out at 77 K, to prevent heating of the sample during the bombardment. Thereafter the samples were heated back to room temperature.

III. RESULTS

We have studied dilute gold-erbium alloys prepared as described in Section II. In the following we shall refer to samples cold-worked by rolling at room temperature, which did not receive any other treatment, as "rolled" samples, and to those samples which underwent a thermal treatment for 1 hour at 400C as "heated" samples. Any other treatment will be pointed out separately. Typical EPR spectra at 1.65K of a "rolled" and a "heated" sample of Au doped with 1000 ppm Er are shown in Figs. 1a and 1b, respectively. The EPR linewidths ΔH were determined according to a procedure outlined in Ref. 4. The EPR linewidth of a paramagnetic ion in a metal host, as a function of temperature T, can be expressed as $\Delta H = a + bT$, where a represents the residual linewidth and b the thermal broadening of the linewidth (the Korringa relaxation rate). To determine a and b, EPR spectra were recorded at several temperatures between 1.65 to 4.2K. The results were plotted as in Fig. 2. The solid lines are least square best fits to the experimental points. The intercept of the solid line with the y axis (extrapolation to 0 K) defines a and the slope of the solid line defines b.

The residual linewidths of "rolled" samples of Au with Er are shown as a function of Er concentration (c) in Fig. 3. From this figure we obtain $a_r = (8 + 16 \times 10^{-3} c)$ Gauss.

From the recorded spectra we also determined the asymmetry parameter A/B (the ratio between the maximum and minimum of the first derivative of the EPR absorption line, for a definition see Fig. 1a). The A/B ratio of "rolled" samples of Au with Er as a function of Er concentration is shown in Fig. 4. The A/B ratios of "rolled" samples are seen to fall between 2 and 3, which is close to the theoretical value[5] of 2.7 for an impurity with a Lorentzian line shape in a thick sample in the diffusionless limit ($T_D/T_2 \to \infty$, where T_D is the time it takes the magnetization to diffuse through the skin depth δ and T_2 is the electron spin relaxation time). The slight concentration dependence of the A/B ratio in "rolled" samples can be expressed as $A/B = 2 + 0.6 \times 10^{-3} c$.

The thermal treatments described, namely heating the samples for 1 hour at 400C in vacuum, air, argon, or hydrogen, cause drastic changes in residual linewidths, as well as in lineshapes (A/B ratios), as can be seen in Fig. 1 for a typical sample of Au with 1000 ppm Er. The thermal treatment decreases the residual linewidth, increases the A/B ratio and also decreases the intensity of the EPR line, where the intensity I is expressed as $I = (A + B)(\Delta H)^2$. The residual linewidth of the "heated" samples, plotted as a function of concentration in Fig. 3, shows the strong reduction in the residual linewidth. We obtained a value of 3.5 Gauss for the residual linewidth of "heated" samples, extrapolated to zero concentration. This, to the best of our knowledge, is the narrowest residual linewidth reported for an

impurity in a polycrystaline metal at X-band frequency. It should be pointed out that this reduction in linewidth is accompanied by a decrease (of 50-90%) in the intensity of the EPR line. A conclusion which can be drawn from this result is that the number of Er ions contributing to the EPR line is less than before heating the samples. The residual linewidth of Er in Au as a function of concentration for "heated" samples can be written as $a_h = (3.5 + 10x10^{-3}c)$Gauss.

The effect of heat treatment on the A/B ratio is shown in Fig. 4. The A/B ratios plotted were extracted from the same EPR recordings for the respective concentrations of Er as the residual linewidths. A slight inconsistency in the A/B values was also observed as a function of temperature in the range of our measurements between 1.65 and 4.2K. Therefore in Fig. 4 an average of the A/B ratio for each concentration was plotted in the above temperature range. A strong increase in the A/B ratio as a function of concentration is observed in the heated samples compared with the "rolled" samples, e.g. for a sample with a nominal concentration of 2000 ppm, we obtained an increase in A/B from 3 in the "rolled" samples to 8 in the "heated" samples. The concentration dependence of the A/B parameter in "heated" samples can be written, from Fig. 4, as $A/B = 2.7 + 2.5x10^{-3}c$.

We studied the possibility of reversing the effects obtained by heat treatment and found the following four ways in which the residual linewidths, the A/B ratios and the intensities of the "heated" samples can be fully or partially recovered to the values observed in the "rolled" samples before the heat treatment: mechanical polishing, deformation by rolling, etching and ion implantation.

Mechanical polishing: A few microns were removed from the surface of a "heated" sample by polishing the side pasted to the cavity during the measurements. Care was taken to protect against direct mechanical damage to the other side of the sample, which is measured by EPR. A 600 grit special silicon carbide wet grinding paper was used for the polishing. This treatment resulted in recovery of the residual linewidths, A/B ratios and intensities to values observed in the sample before the heat treatment. An increase in the linewidth after mechanical polishing has to be expected, since similar to rolling or filing it also introduces dislocations in metals.

Deformation by rolling: A sample of Au with a nominal concentration of Er of 1000 ppm and a thickness of 0.75mm was prepared by rolling. The EPR spectrum exhibited the regular features of the "rolled" samples reported above. Then the sample was heated in vacuum (1 hour at 400C). The EPR spectrum after the heat treatment again exhibited the regular features of the "heated" samples. Thereafter the sample was successively rolled down to thicknesses of 0.53, 0.25 and 0.15mm. The EPR spectrum was recorded after each rolling. The residual linewidths and the A/B ratios are plotted in Fig. 5 as a function of the cold-work $\Delta h/h_o$. Here $\Delta h = h_o - h_i$, $h_o = 0.75$mm, is the thickness of the sample before the successive rolling, and h_i is the thickness of the sample after the i-th rolling step. Successive recovery of the linewidth and of the A/B ratio are clearly demonstrated in this figure. The residual linewidth and

the A/B ratio of the 0.75mm thick "rolled" sample were 26.4G and 2.6 respectively. Thus one can see from Fig. 5 that for $\Delta h/h_o = 0.8$ most of the linewidth and A/B ratio were recovered. The intensity of the resonance line (I) and the concentration of Er ions (c) in the skin depth increased as a function of cold-work. The behavior of I and c as a function of $\Delta h/h_o$ is summarized in Table I.

Etching: The etching experiments were carried out to determine whether or not the heat treatments are surface effects. An Au sample with a nominal Er concentration of 2000 ppm was etched successively in dilute aqua regia ($HCl:HNO_3:H_2O$ = 3:1:2). The thickness of the etched-off layer was determined by accurate weighing of the sample. The results are plotted in Figs. 6 and 7 showing the recovery of the linewidth and A/B ratio respectively, as a function of the thickness of the etched-off layer. The linewidth and A/B ratio at 1.65K of the "rolled" sample before heating and etching were 52G and 3 respectively. Thus one can see from Fig. 6 that etching-off 5000 Å of the surface of the sample recovers about 80% of the linewidth and no appreciable recovery is obtained by increasing the etched-off layer to 2 microns. On the other hand Fig. 7 demonstrates full recovery of the A/B ratio after etching-off 5000 Å. After etching, most of the intensity was recovered.

Ion Implantation: Three types of ion implantation experiments were carried out: (a) implantation of Ar ions in rolled samples with doses of $\approx 10^{15}$ and $\approx 10^{16}$ ions/cm^2 at room temperature. No effect

was observed after this implantation; (b) implantation of Ar ions in heated samples with a dose of 2.5×10^{16} Ar ions/cm^2; (c) implantation of Au ions in heated samples with a dose of 2×10^{16} Au ions/cm^2. During (b) and (c) samples were kept at 77K and after implantation were heated to and kept at room temperature until the EPR experiment. In both cases partial recovery of the linewidth, intensity and A/B ratio was observed as compared with values recorded before heating. The results are summarized in Table II. It should be pointed out, that the maximum penetration depth of the Ar and Au ions in Au at 340 keV(the maximum energy used for the implantation) is 900 and 300 Angstroms, respectively.

Computer best fits and calculations of the EPR lineshapes were performed. We found that the lineshapes of the rolled as well as heated samples can be fitted quite well by using a Lorentzian lineshape, with the following four fitting parameters: linewidth ΔH, percent dispersion (determines the A/B ratio (% dispersion + % absorption = 100%), the resonance field H_o (determines the g-factor), and the intensity. A computer fitted first derivative of the central absorption line of 1500 ppm Er in Au in a rolled sample is shown in Fig. 8. The fit also includes the hyperfine structure contribution. The experimental points used for the fitting were extracted manually from the recorded EPR spectrum. The fitted parameters obtained are given in Table III. In the upper part of Fig. 9 the whole computer calculated spectrum of Er is shown. The fitted parameters of Fig. 8 were used for this calculation and the experimental points are plotted as open circles. In the lower curve

of Fig. 9, a whole experimental spectrum is shown for comparison. The fit seems very good. In Fig. 10 we show a computer fitted first derivative of the central absorption line of 1500 ppm Er in Au in a heated sample. The spectra of the same sample rolled are shown in Figs. 8 and 9. The fitted parameters for this spectrum are also given in Table III. The upper curve of Fig. 11 is a computer calculated whole spectrum (including the hyperfine structure) of the heated sample of Fig. 10, using the same data points and the same fitted parameters. The lower curve is an experimentally recorded EPR spectrum of the same heated sample. One can see here too that the fit is very good.

During this study it proved useful to have a graph of the A/B ratio as a function of the admixture of the absorption and dispersion. We calculated this relationship for a Lorentzian lineshape (which gives a very good fit with our experimental results), for a single EPR line without a hyperfine structure, and we show the relationship in Fig. 12. The extreme cases, A/B = 1 and A/B = 8 for 100% absorption and 100% dispersion respectively, were mentioned previously in the literature[6].

The A/B ratio observed experimentally in a recorded EPR spectrum which also has a hyperfine structure can deviate considerably from the A/B ratio for the same admixture of absorption and dispersion, when there is no hyperfine structure present. This effect is especially pronounced for large linewidths and large A/B ratios. We have calculated the deviations of the A/B ratios due to the hyperfine

structure, as a function of the linewidth ΔH for the case of Er with a Lorentzian lineshape. The results are shown in Fig. 13. To the best of our knowledge, this point has never been treated in the literature. It turned out that for most cases the deviations were within the experimental accuracy of the determination of the A/B ratio, since for large A/B values (heated samples), the linewidths were narrow. There are,however, other real physical cases (e.g. Yb) where this effect can be of importance.

In the course of this work, we found it useful to know the skin depth as a function of Er concentration in Au. For a general case the skin depth δ, defined as that distance below the surface of a conductor where the current density has diminished to 1/e of its value at the surface, is given as[7]

$$\delta = (\lambda_o \rho / \pi \mu_o c_o)^{\frac{1}{2}} \text{ meters}$$

where λ is the wavelength of the radio frequency microwave radiation (in our case, ν = 9.4 GHz, thus $\lambda_o = 3.1894 \times 10^{-2}$m).

ρ is, in a general case, the resistivity of the conductor. In our case, since the experiments were carried out at 4.2K or below, ρ is the residual resistivity (in Ω m).

μ_o is the premeability, $\mu_o = 4\pi 10^{-7} \mu_r$henry/m

μ_r is the relative permeability of the conductor (for non-magnetic materials $\mu_r = 1$).

c_o is the velocity of light (2.998×10^8 m/sec).

Our resonance experiments were all carried out at approximately the same resonance frequency ($\nu \simeq 9.4$ GHz), and at temperatures between

1.65 and 4.2K. Thus the skin depth is determined by the residual resistivity of the sample. The dominant contribution to the residual resistivity is due to the Er doping. We have used the value $\rho \approx 7\mu\Omega cm/at.\%$ Er[8] for our calculations. The contribution of the residual resisitivity of pure Au is very small compared with the resistivity at our Er doping levels ($\rho_{Au(pure)} \sim 1.2$ nΩcm, see e.g. Ref. 9). The skin depth δ and the residual resistivity ρ in Au doped with Er, as a function of the concentration of Er, were calculated and are presented in Fig. 14.

We also tried to check the possibility of affecting the spin lattice relaxation time T_{sl} by codoping with a spin scatterer. Sb was chosen as the codopant, which was found to be very effective in the Ag:Mn system[10]. Samples of Au + 300 ppm Er + 100 ppm Sb, Au + 1000 ppm Er + 300 ppm Sb, and Au + 1000 ppm Er + 1000 ppm Sb were prepared. However no significant changes in the linewidth or lineshape in these samples, either rolled or heated, were observed. Dahlberg[11] studied the Ag:Er system using In,Sn,Y,Lu and Sb as codopants and found that Y and Lu increased the linewidth significantly. He attributed this broadening as being due to Kohn-Vosko type oscillations in the charge density.

As mentioned above, the heating of the samples produced a decrease in the integrated intensity of the resonance line and thus also a decrease in the number of spins (the "effective concentration" of Er^{3+} in the skin depth) contributing to the resonance line. We

found that this decrease is almost independent of the doping level. For doping levels between 300 and 2000 ppm the "effective concentration" of Er^{3+} in the samples heated for 1 hour is (25±13)% of its value before heating. Preliminary investigations indicate that this decrease seems to reach a minimum, since no appreciable difference in the concentration was observed between samples heated for 4 hours and 8 hours, the concentration being (8±4)% of its value before heating.

IV. THEORY[12]

A. Introduction

In order to interpret the experimental results we need an understanding of the behavior of the EPR linewidth ΔH after heat treatment and of the changes in the lineshape (the asymmetry parameter A/B) after heat treatment, as well as of a slight concentration dependence of A/B before heat treatment.

In principle the dynamic equations of the Bloch-Hasegawa[13] type have to be solved for our specific case. This approach is restricted by a large number of parameters which enter the equations, some of which are not well known (e.g. the T_{s1}^{-1} before and after heating; T_{s1} is the spin lattice relaxation time of the conduction electrons due to mechanisms other than the s-d exchange). However, these equations are also restricted by their nature:

a) They do not take into account the real Fermi surface, which may deviate very significantly from a simple sphere. (In other words, these equations do not take into account the spread of the g-factors

of conduction electrons over the $\vec{k}$-space on the Fermi surface) Effects of this spread may be significant if there are large enough regions where the $g(\vec{k})$ factors are near the 6.8 value of Er^{3+} and when there is intensive electron-electron scattering between electrons with very different g-values. We will return to this question in the following discussion, but is seems that for Au there are no electrons with $g(\vec{k})=6.8$, or electrons with $|g(\vec{k})-6.8| << |\lambda\chi_s g_s + \frac{\Delta H}{H}|$ (all the electron g-values are near 2).

b) The other restriction of the Bloch-Hasegawa type equations is due to the existence of a residual linewidth at zero Er concentration. This "single ion" residual linewidth cannot be attributed to the phonon broadening. It can be understood by considering local deformation due to random stress present in the metal because of dislocations. In this case the real lineshape is a convolution of the "intrinsic" lineshape and of the stress distribution. ΔH follows the equation $\Delta H=a+bT$, which suggests the existence of a Lorentzian - Lorentzian convolution. This type of convolution gives a sum of the widths. It is included in a.

The spin-spin width is included in the Bloch-Hasegawa equations in the phenomenological way. The parameter T_{dl}^{-1} in the Bloch-Hasegawa equations is used to describe a channel, independent of relaxation of the conduction electrons[14,15]. Instead of T_{dl}^{-1}, which does not have a theoretical basis in the case of metals, we use another parameter, T_{dd}^{-1}, which describes the concentration dependent part of the linewidth ΔH.

Another complication is caused by the experimental results which show that heating seems to affect a surface layer of the order of 6000 Å, which is also the skin depth for a 2000 ppm sample. Hence our

signal comes from a layer on the surface of the metal, which is different from the rest of the bulk (after heating). This may also be a cause of the deformation of the lineshape.

Finally, the deformation of the EPR line from the ($\chi''+\chi'$) form (A/B≈2.7) is attributed traditionally to the influence of the conduction electrons. One may check if some (new) mechanism exists which may provide effective diffusion of the Er^{3+} transversal magnetization (after heating). One hypothesis will be described below.

The question is whether one or more of the following three mechanisms can be responsible for the changes in the A/B ratio after heating: the conduction electron influence, an inhomogeneous structure of the upper region of the metal, the diffusion of the Er^{3+} magnetization (which may be induced by electrons).

It was proposed that the following experiment might clarify the first point mentioned above. Sb is known to be an efficient scattering center[10], i.e. the effect of Sb doping is to increase the spin-flip relaxation rate of the conduction electrons via spin-orbit scattering. *It was expected that codoping of Au:Er samples with 100-1000 ppm Sb* should not affect the lineshape in the rolled samples (before heating). This would prove that the influence of T_{sl}^{-1} on the Er^{3+} resonance before heating is negligible. If, after heating, the lineshape of the Sb doped samples does not differ from the shape of heated samples without Sb, then our case is not a "combined" resonance case (hybrid-resonance, strong coupling case). As described in section III, no significant changes were detected in rolled or heated samples of Er doped Au, codoped with Sb. This, together with the fact that $g_e \ll g_{Er}$, indicates that the model of a combined resonance must be rejected.

B. The linewidth and g-shift

The linewidth can be expressed as

$$\Delta H = DH_o + DH_c + DH_K$$

where DH_K is the Korringa contribution to the linewidth ($DH_K = bT$). Our experimental results indicate that DH_K does not depend on the heat treatment. $DH_K \simeq 2.5T$ G/°K. DH_c, the Er concentration dependence of the linewidth, is a linear function of the concentration. This contribution is believed[16] to be a spin-spin and a Kohn-Vosko[17] contribution to the linewidth. This part also gives information on the number of Er spins contributing to the resonance line. DH_o is the true residual linewidth due to random stresses.

1) DH_K

Since the lineshape before heating is of the simple localized moment form ($A/B \simeq 2.7$) and the hyperfine structure is well resolved, we conclude that DH_K is of the non-bottleneck type, so that

$$DH_K T^{-1} = \frac{\pi}{g_d \mu_B} \langle J^2 \rangle \eta^2 k_B \qquad (1)$$

and for $DH_K T^{-1} = 2.5$ G/°K

$$\sqrt{\langle J^2 \rangle}\ \eta = 0.019 \qquad (2)$$

where[10,18] $\langle J^2 \rangle = \left\langle \frac{J(q)^2}{(1 - U(q)\chi(q))^2} \right\rangle$.

Introducing $\sqrt{\langle J^2 \rangle} = J_{eff}$, we obtain for the exchange parameter for $\eta = 0.15$ eV^{-1} per atom per spin

$$J_{eff} = 0.13 \text{ eV}. \qquad (3)$$

$U(q)$ is the electron-electron Coulomb interaction responsible for the exchange enhancement of the conduction-electron susceptibility. $J(q)$ is the q-dependent exchange interaction; $J(0)$ is the $q = 0$ component; $\chi(q)$ is the q-dependent static susceptibility; $\chi(0)$ is the $q = 0$ component. The symbol $\langle\ \rangle$ means the normalized sum from $0 \leq |q| \geq 2k_F$.

The other estimation of the related parameter is obtained from the g-shift Δg. We know that in the non-bottleneck regime the shift of the g_d-factor is equal to

$$g_d = g_d^o \lambda \chi_s \simeq \frac{1}{2} g_s J'_{eff} \rho \left(= \frac{1}{2} g_s J'_{eff} \rho \frac{1 + \lambda \chi_{sd}^o}{1 - \lambda^2 \chi_s^o \chi_d^o} \right) \qquad (4)$$

χ_s is the conduction electron spin susceptibility,

where $J'_{eff} = \dfrac{J(0)}{1 - U(0)\chi(0)} \simeq J(0)$ (see Ref. 18.)

(This equation is a good enough approximation for estimation purposes.)

For the effective field $J = J(0)$, λ is

$$\lambda = \frac{J}{g_s g_d \mu_B^2 \frac{N'}{V}} \qquad (4')$$

$$\chi_s = \frac{1}{1 - U(0)\chi_s^o(0)} \chi_s^o \frac{1 + \lambda \chi_d^o}{1 - \lambda^2 \chi_s^o \chi_d^o} \simeq \chi_s^o \frac{1 + \lambda \chi_d^o}{1 - \lambda^2 \chi_s^o \chi_d^o} \qquad \text{and}$$

$\chi_s^o = \frac{1}{2} g_s^2 \mu_B^2 \eta \frac{N'}{V}$ is the Pauli susceptibility, where N' is the number of atoms per unit cell and V is the volume of the unit cell, $\frac{N'}{V} = \frac{4}{a_o^3}$ for Au, $a_o = 4.07$ Å, thus $\frac{N'}{V} = 5.93 \times 10^{22} cm^{-3}$.

$\chi_d^o = c \frac{\eta_d^2 \mu_B^2 S(S+1)}{3k_B T} \frac{N'}{V} \simeq c \frac{\eta_d^2 \mu_B^2}{4k_B T} \frac{N'}{V}$ is the susceptibility of the Er^{3+}.

In general $J_{eff} \neq J'_{eff}$, but for estimation purposes one may ignore this difference (up to a factor of 2).

To estimate $\lambda\chi_s \simeq \lambda\chi_s^o$, the parameter which enters the Bloch-Hasegawa equations, we use Eq. 4.

$$\lambda\chi_s = \frac{\Delta g}{g_d^o}$$

$g_d^o = 6.80$ assuming Russel-Sounders coupling and 6.77 if deviations from Russel-Sounders coupling are taken into account[19]. If we take (somewhat arbitrarily) $\Delta g \leq 6.80 - 6.77 = 0.03$, we obtain

$$\lambda\chi_s \simeq \frac{0.03}{6.8} = + 4.4 \times 10^{-3} \qquad (5)$$

For $\chi_s \simeq \chi_s^o \simeq 10^{-6}$ (for $\eta = 0.15$ eV^{-1}), using Eq. 4, we obtain

$$\lambda \leq 4.4 \times 10^3 \qquad (6)$$

$$J'_{eff} \leq 0.1 \text{ eV}, \quad J \leq 0.1 \text{ eV} \qquad (7)$$

The values in Eqs. 7 are in good agreement with Eq. 3. From this estimation we can see that $(1 - \lambda\chi_s^o\chi_d^o) \simeq 1$, and

$$\Delta g_d = J'_{eff}\eta(1 + \lambda\chi_d^o) = J'_{eff}\eta(1 + \lambda c\frac{const.}{T}) \qquad (8)$$

where c is the Er concentration and $const. = \frac{g_d^2\mu_B^2}{4k_BT}\frac{N'}{V} = 0.427$ per ppm Er $= 4.27\times10^{-4}$ per 1000 ppm Er.

There are no accurate measurements available for $g = f(c,T)$ for Er^{3+} in Au. At T = 1.65K, it seems that for between 100 and 600 ppm Er the g-factor does not change ($g \simeq 6.74$) while it increases slightly in the range from 600 to 2000 ppm Er ($g_{1000} \simeq 6.75$, $g_{1500} \simeq 6.77$, $g_{2000} \simeq 6.78$).

From Eq. 8 we obtain

$$\frac{\Delta g_{2000} - \Delta g_{1000}}{\Delta g_{1000}} \simeq \lambda\frac{4.3\times10^{-4}}{T} = 3\times10^{-2}.$$

Using the above value, we obtain for λ

$$\lambda \simeq \frac{3T}{4.3} \times 10^2 \simeq 10^2 \qquad (9)$$

However, from Eq. 6 we have $\lambda \leq 4\times10^3$. The difference between Eqs. 6 and 9 is too large, probably because some of the data are not accurate enough. Either $\Delta g_{2000}-\Delta g_{1000}$ is larger than 0.03, or the Δg taken in Eq. 5 is too large, or χ_s is much larger than χ_s^o. In any case, the difference between J_{eff} and J'_{eff} (see Eqs. 1, 2 and 4) is of the order of 2. Hence Eq. 3 gives a good estimate of λ which is in agreement with Eq. 6.

2) DH_c

The concentration dependent contribution to the linewidth DH_c was discussed by Dahlberg[16] for the case of Ag:Er.

$$DH_c = DH_{SS} + DH_{KV}$$

DH_{SS} is the spin-spin part of DH_c. This is the homogeneous contribution. If $c << 10^4$ ppm, the DH_{dd} contribution to the linewidth for the random location of the impurity can be estimated from Kittel and Abrahams paper[20]. For S = 1/2 only the dipole-dipole part contributes (the isotropic exchange does not contribute for the S = 1/2 case when c is small enough).

Using the second and fourth moments of the EPR spectrum one can write

$$DH_{SS} = \frac{\pi}{2\sqrt{3}} \frac{\langle \Delta\nu^2 \rangle^{3/2}}{\langle \Delta\nu^4 \rangle^{1/2}} \frac{1}{g_d \mu_B} \qquad (10)$$

(Eq. 10 is not exact, because one would have to define the width for some configuration of Er and after this to average the lineshape for the random case. This is a difficult procedure.)

Behringer[21] calculated the averages of the second and fourth moment $\overline{\langle \Delta\nu^2 \rangle}$ and $\overline{\langle \Delta\nu^4 \rangle}$ respectively. Using his calculation one obtains

$$DH_{SS} = \frac{c}{1000 \text{ ppm}} 12.5 \text{ G} \qquad (11)$$

Here c is in ppm.

The other concentration dependent part is the Kohn-Vosko contribution

$$DH_{KV} \propto cf \tag{12}$$

where f is the frequency.

For Ag:Er Dahlberg[16] obtained the following experimental results at a frequency of 9.4 GHz:

$$DH_{KV} = \frac{c}{1000}\,(19.7 \pm 7.5)\,G$$
$$DH_{SS} = \frac{c}{1000}\,(8 \pm 5)\,G \tag{13}$$

Our results indicate that DH_{KV} for Au:Er must be much smaller than in Ag:Er. From Fig. 3 we obtain for rolled samples

$$DH_c \simeq \frac{c}{1000}\,16\ G \tag{14}$$

If we take the theoretical value for the dipole-dipole part, we obtain $DH_{KV}^{estimated} \simeq \frac{c}{1000}\,4\ G$

DH_{SS} in Au must be the same as in Ag. If we adopt Dahlberg's[16] value of $\sim$ 8 G/1000 ppm given in Eq. 13 above, we obtain:

$$DH_{KV}^{estimated}(Au) \simeq \frac{c}{1000}\,8\ G$$

This value is also much smaller than that obtained by Dahlberg[16] for Ag (given in Eq. 13 above). This indicates that Er^{3+} produces much less distortions in Au than in Ag. The same conclusion can also be drawn from the residual linewidth extrapolated to zero concentration, which is 8 G for Er in Au (rolled samples, see Fig. 3) and 14.5 G for Er in Ag[16] (samples were prepared by filing of the arc melted pellet.)

Now we will make a crude estimation of the number of Er ions (number of spins in %) contributing to the resonance line after heating. From our experimental results we have:

$$DH_c(\text{rolled}) = 16 \frac{c_i}{1000} G$$
$$DH_c(\text{heated}) = 10 \frac{c_i}{1000} G \qquad (16)$$

Here c_i is the initial concentration of Er^{3+} in the rolled samples before heating. If we neglect the contribution to the DH_c(heated) of the Er ions trapped on dislocations, we have

$$10\, c_i = 16\, c_f \qquad (17)$$

(because in our model the EPR signal is due to randomly distributed Er^{3+} ions which do not sit on dislocations). From this it follows that:

$$c_f = \frac{10}{16} c_i, \qquad (18)$$

thus $c_f \approx 0.62\, c_i$. c_f is the final concentration of Er^{3+} contributing to the resonance line after heating. This means that only 62% of the spins would contribute to the EPR signal if the influence of the trapped Er^{3+}(on the dislocations) on the width DH_c is negligible. But apparently this is not the case. We suppose, that the valence state of Er on the dislocations is also 3+, so that they produce dipolar and exchange fields on the randomly distributed Er^{3+}.

It is difficult to estimate this effect because if there is clustering of Er^{3+} at the dislocations, the ground state of a cluster may be non-magnetic (for the antiferromagnetic type of exchange).

Without a concrete model of the clusters, we can not say anything about the values of the dipolar and exchange fields which the trapped Er produces on the sites of the randomly distributed Er.

If we assume that all Er ions effective in the Kohn-Vosko mechanism produce roughly the same width (4 + 8 G per 1000 ppm) as before heating, then half or more of the 10 G per 1000 ppm width is due to the Kohn-Vosko mechanism. In this case we have instead of Eq. 18 either $(10 - 4)\ c_i = 12\ c_f$

$$c_f = \frac{6}{12}\, c_i,\ c_f = 0.5\ c_i \tag{19}$$

or

$$(10 - 8)\ c_f = 8\ c_i,\quad c_f = 0.25\, c_i. \tag{20}$$

Thus 25% to 50% of the Er^{3+} are not trapped on dislocations after heating. The lower value (25%) is in good agreement with the experimental results.

Another model, opposed to the above mentioned one, would be to assume a sharp increase in the concentration of Er in a surface layer after heating, with $c \gtrsim 10{,}000$ ppm. This would result in i) a decrease in the linewidth due to the effect of Van Vleck narrowing and ii) diffusion of the Er magnetization, occurring because of the interaction between the Er ions. The lineshape would be Dysonian with $A/B > 2.7$, and also the A/B ratio would increase with increasing concentration of Er. In this model it is expected that with the χ of the exchange narrowed form, the shape of the resonance line ($P \propto \chi' + \chi''$) would be mainly Lorentzian and

Gaussian in the wings. We do not elaborate on this model here because it is not consistent with the experimental results obtained after polishing the samples, where full recovery of the lineshape, linewidth and intensity was obtained, which opposes the assumption of a surface layer with a sharp increase in Er^{3+} concentration.

3) DH_o

This contribution to the residual linewidth is a function of the random stresses, which originate from the non-Er impurities and from dislocations. Since the purity of the Au used in our experiments is 99.999%, the concentration of all the other impurities is approximately 10 ppm. Thus they would represent only a relatively small part of DH_o. Assuming that the dislocations are responsible for most of DH_o, we can understand why DH_o decreases after heating (from ≈8 to ≈3.5 Gauss, see Fig. 3). It is well known, that dislocations move through the metal during heating, dislocation lines also move during this process and the grain size increases, and therefore the number of dislocations near Er ions also decreases.

C. The A/B ratio (the lineshape).

1) In the rolled samples the A/B ratio changes slowly from A/B=2 for $c \to 0$ to A/B=3 for c = 2000 ppm (see Fig. 4). The theoretical value of the A/B ratio for an impurity in a metal in the diffusionless limit is 2.7. There may be several reasons for this small deviation from the theoretical value. After heating the A/B ratio increases (see Fig. 4.). This effect is especially pronounced for

large concentrations of Er (c = 1000 + 2000 ppm). One must explain both the small concentration dependence of A/B in the rolled samples, as well as the increase in the A/B ratio after heating.

2) We discuss the possibility that the A/B ratio after heating is caused by the random ensemble of the Er^{3+} resonances with anisotropic g-factors. If after heating the g-factor became anisotropic with a random distribution of Δg, a broadening of the resonance line would result. However experimentally we observe a narrowing of the resonance line after heating.

3) In this discussion we dismiss the straight forward influence of the conduction electrons, for the following reasons:

a) Since

$$|g_s - g_d| > |\lambda \chi_s g_s + \frac{\Delta H}{H}| \qquad (21)$$

we cannot expect that the resonance is a sort of combined d-electron-conduction-electron resonance.

b) We do not expect that an enhancement of the H_1 field via the λM_s term will change the lineshape drastically due to Eq. 21 (see ref. 15.). The experimental results indicate that there is no difference between the high-field and low-field hyperfine components. If λM_s were essential, the high-field and low-field enhancements would not be expected to be the same.

c) If $T_{sl}^{-1} \approx T_{sd}^{-1}$, a bottleneck in the relaxation may result. It is hard to imagine that this could occur for concentrations of c ≈ 1000 ppm. After heating, T_{sl}^{-1}, may only be smaller, because the number of the dislocations decreases. But also T_{sd}^{-1} - which

is proportional to the concentration - becomes smaller (T_{sd} may be shorter than T_{sl}).

d) If the concentration increases then the resistance $1/\sigma$ also increases. The diffusion coefficient of the conduction electrons is $D_e = (1/3)V_F^2\tau$, where τ is the collision time which determines the conductivity and V_F is the electron velocity at the Fermi surface. The diffusion coefficient D_e decreases with the increase of concentration. The conduction electron lineshape becomes more symmetric with smaller D_e (larger c). We cannot explain how the more symmetric conduction electron line can cause the asymmetry of the Er resonance.

From the qualitative and semiquantitative arguments we can assume that there is no direct dynamic influence of the conduction electrons on the Er^{3+} resonance. The conduction electrons serve mainly as a thermal bath and cannot change the A/B ratio of the Er^{3+} resonance with increasing concentration of Er.

D. *Diffusion due to the spin-spin interaction.*

If there is diffusion of the magnetization due to the spin-spin interaction, we have to add to the Bloch equation the diffusion term

$$D\Delta\vec{M} \qquad (22)$$

This term, if it exists, leads to the same A/B ratio as in the case of the conduction electrons, because $A/B = f(R)$, where $R = \delta/\sqrt{DT_2}$

is the parameter of the Dysonian lineshape. In the case of the conduction electrons the A/B ratio as a function of R assumes values between 2.7 and 18.

In nuclear magnetic resonance (NMR) treatises the diffusion of the nuclear population via the spin-spin interaction is discussed.

$$D_d \simeq \frac{1}{30} \cdot \frac{a_o^2}{T_2} \rightarrow \simeq \frac{c^{-2/3}}{c^{-1}} \simeq c^{1/3} \qquad \text{(if } c \ll 10000 \text{ ppm)} \qquad (23)$$

where a_o is the distance between adjacent spins and T_2^{-1} is the half width. This diffusion is caused simply by flip-flop (see Ref. 22). The T_2 is the time of the loss of the coherence of two adjacent spins. If the interaction passes the spin-population from spin to spin, the same interaction (dipole-dipole) may cause the diffusion of the M_Z component of the magnetization. We have to include in Eq. 23 only the spin-spin interaction

$$T_2^{-1} = (T_2^{-1})_{dd} + (T_2^{-1})' \qquad (24)$$

where $(T_2^{-1})' = (T_2^{-1})_{\text{Korringa}}$ + other sources of broadening. Thus we obtain

$$\delta_M = (D_d T_2)^{\frac{1}{2}} \simeq (D_d T_d \frac{T_2}{T_d})^{\frac{1}{2}} = (a_o^2/30)^{\frac{1}{2}} (T_2/T_d)^{\frac{1}{2}} =$$

$$(a_o/\sqrt{30})\ c^{1/3}\ \sqrt{(T_d)^{-1}/(T_d^{-1} + T^{-1}_{\text{Korringa}})} \qquad (25)$$

Since $T_d^{-1} \propto c$, $c^{-1/3}\sqrt{T_d^{-1}} \propto c^{1/6} \rightarrow 0$ if $c \rightarrow 0$ (in the case that $T_D^{-1} \ll T^{-1}_{\text{Korringa}}$).
For $c=10^3$ ppm and T = 1.65K:

$(T_d)^{-1}/(T_d^{-1} + T^{-1}_{\text{Korringa}}) \simeq 12/17 = 0.7$, $\sqrt{0.7} \simeq 0.83$.

$a_o = 4.1$ Å

$\delta_M \simeq 50$ Å $\ll \delta = 4300$ Å

$\delta/\delta_M \simeq 80 \gg 1$, and $A/B \simeq 2.7$

Thus there is no influence on the lineshape for this case.

For $c \gg 10{,}000$ ppm, $\sqrt{(T_D)^{-1}/(T_D^{-1}+T^{-1}_{\text{Korringa}})} \simeq 1$ and $\delta_M \to a_o$. Here, there is also no influence on the lineshape. Therefore for all c, $\delta_M/\delta \ll 1$ and there is no influence on the lineshape.

E. Diffusion due to other mechanisms

We now consider whether or not there are other mechanisms of the spin-diffusion of Er which do not depend upon the Er-Er interaction. It seems that the electron diffusion must also lead to the diffusion of the M_x magnetization, although a detailed calculation is not available. (This diffusion term may arise from the interference term between the electron diffusion term and the electron - local spin interaction term in the density matrix formalism of the linear response. The qualitative arguments are as follows.

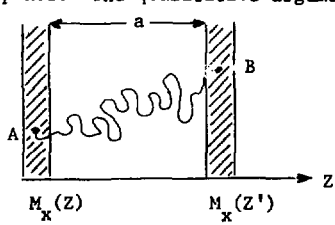

Electrons take the M_x component from the local spin at the point A (relaxation of the x component of the magnetization) and because of the diffusion of the electrons return part of the magnetization at the point B.

The effective diffusion coefficient for the M_x of Er will be of the order of

$D_e \frac{T_{sd}^{-1}}{T_{sd}^{-1} + T_{sl}^{-1}}$ x(loss of the magnetization to the lattice for the time a_o^2/D_e),

where D_e is the diffusion coefficient of the electrons, $D_e \simeq \frac{1}{3} V_F^2 \tau$,

$\delta_{1000ppm} \simeq 10^{-13}$ sec, $\tau \simeq 10^{-14}$ sec/at.% Er and $\frac{T_{sd}^{-1}}{T_{sd}^{-1} + T_{sl}^{-1}}$

is the probability of returning the magnetization to the Er. If

the $\frac{a_o^2}{D_e}$ time for the adjacent Er is much smaller than T_{sl}, we ignore

this correction to the losses. For 1000 ppm:

$$a_o^2/D_e \simeq \frac{(4\text{Å})^2 x 10^{-16} \ (1000)^{2/3}}{6x10^2} \simeq 10^{-16} \text{ sec} << 10^{-10} \text{ sec.}$$ It follows that

$$D_{Er}^{induced} \simeq D_e \frac{T_{sd}^{-1}}{T_{sd}^{-1} + T_{sl}^{-1}}$$

$$D_{Er}^{induced} \simeq D_o (1/c) \frac{(T_{sd}^{-1})_o \, c}{(T_{sd}^{-1})_o \, c + T_{sl}^{-1}} = D_o \frac{1}{c + (T_{sl}^{-1})/(T_{sd}^{-1})_o}$$

because $D_e \simeq \tau \simeq \frac{1}{c}$

and $$\delta_M = \left(D_o \frac{1}{c + (T_{sl}^{-1})/(T_{sd}^{-1})_o} T_2 \right)^{1/2} \qquad (26)$$

Since $T_2 \simeq 1/c$, it follows that

$$\delta_M \propto 1/c^{1/2} \left(\frac{1}{c + (T_{sl}^{-1})/(T_{sd}^{-1})_o} \right)^{1/2}$$

If $T_{sl}^{-1} \propto c$, δ_M decreases with the increase of the Er concentration. This means that the parameter $R = \delta/\delta_M \simeq \frac{c^{1/2}}{1/c} = c^{3/2}$ increases with c and the A/B ratio must decrease, which contradicts the experimental results. Hence this mechanism cannot explain the increase of

the A/B ratio with the increasing concentration of Er. In addition one also has to explain why δ_M increases after heating.

If (for c = 10000 ppm) $\frac{T_{sd}^{-1}}{T_{sd}^{-1} + T_{sl}^{-1}} \simeq 1/3$

$$\delta_M \simeq (\tfrac{1}{3} D_e T_2)^{\frac{1}{2}}$$

$$T_2^{-1} = \frac{g_d \mu_B \Delta H}{\hbar} = \frac{6.8 \times 9.27 \times 10^{-21} \times 10}{10^{-27}} = 6 \times 10^8$$

$$T_2 \simeq 0.7 \times 10^{-9}$$

$$\delta_M \simeq (5.6 \times \tfrac{1}{6} \times 10^{-8})^{\frac{1}{2}} \simeq 10^{-4} \text{ cm} = 10^4 \text{ Å}$$

$$\frac{\delta}{\delta_M} = R \simeq \frac{0.4 \times 10^4}{10^4} = 0.4$$

The corresponding A/B from Feher and Kip[5] is approximately 7. This value seems to be satisfactory, but the decrease of R with the increase of the concentration cannot be explained on the basis of Eq. 26.

F. The surface impedance in the case of an inhomogeneous Er distribution

The A/B ratio may depend on the degree of homogeneity of the distribution of the Er ions in the sample. The results of the etching experiment suggest the following model. We consider a surface layer with a thickness d, conductivity σ_1 and Er concentration c_1, and the bulk of the sample with a conductivity σ_2 and Er

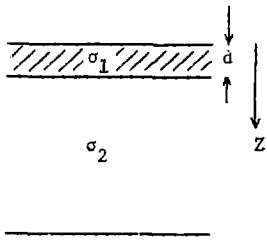

concentration c_2. If $d \lesssim \delta$, the EPR will be a superposition of the signal from the layer d and from the bulk. In addition, a reflection may take place on the interface between the layer d and the bulk.

Upon solving Bloch-like equations[15] for the two media (d-layer and bulk), the power absorbed by the metal sample can be written in the form

$$P_m = H^2_{surface}\ (\omega/4)\left\{\delta_1 \pi \omega_{d_1}\ \chi^o_{d_1}\left[C_{1-}\ \chi'_1(\omega) + C_{1+}\ \chi''_1(\omega)\right] + \right.$$

$$\left. \delta_2 \pi\ \omega_{d_2}\ \chi^o_{d_2}\ \left[C_{2-}\ \chi'_2(\omega) + C_{2+}\ \chi''_2(\omega)\right]\right\}$$

$H_{surface}$ is the rf magnetic field on the surface of the sample. ω_{d_1} and ω_{d_2} are the resonance frequencies for the d-layer and bulk respectively. $\chi^o_{d_1}$ and $\chi^o_{d_2}$ are the static susceptibilities for the d-layer and bulk respectively. The C's are coefficients which depend on the ratios of d/δ and σ_1/σ_2. $\chi'(\omega)$ and $\chi''(\omega)$ are the dispersion and absorption parts of the complex susceptibility, the indexes 1 and 2 refer to the d-layer and bulk, respectively.

Further computations are necessary to develop this model. It is possible that this idea of a combined resonance from two layers of

different concentrations of Er may provide an explanation for the behavior of the A/B ratio.

V. D I S C U S S I O N

We have used the EPR technique to study defects produced in dilute Au:Er alloys by cold-working and ion bombardment. Most of our results,as reported in Section III, concern defects produced by cold-working of the metals. The results obtained on the effects of ion bombardment are preliminary and constitute a small fraction of this work, however they indicate the possibility of a promising opening of an area of research to which the EPR technique could be applied. Our research was concentrated mainly on the study and interpretation of the behavior of the characteristic features of the EPR spectrum. Cold-working and heating of our samples produced changes in the EPR linewidth ΔH, the integrated intensity of the resonance line I(which is proportional to the number of spins contributing to the resonance line) and the lineshape (the asymmetry parameter A/B).

The EPR linewidth ΔH in the temperature range of our experiments is a linear function of temperature and can be written $\Delta H = a + bT$. The Korringa relaxation rate, represented by b, was found to be independent of the Er concentration and of the various treatments. This shows that we have an unbottlenecked system. All changes in the linewidth are contained in the residual linewidth a. In the range of the Er concentrations covered by our experiments, the residual linewidth was a linear function of the concentration for rolled and heated samples as well. The residual linewidth can be

expressed as $a = DH_c + DH_o$. The concentration dependent part DH_c is composed of the spin-spin contribution DH_{SS} and the Kohn-Vosko contribution DH_{KV}. The values obtained for DH_c from our experiments (see Fig. 3) are 16 G/1000 ppm Er and 10 G/1000 ppm Er, for rolled and heated samples respectively. Assuming the same value $DH_{SS} \simeq \frac{c}{1000}$ 8 G obtained for Er in Ag[16], we obtain $DH_{KV} \simeq \frac{c}{1000}$ 8 G for rolled samples. Using the calculated value $DH_{SS} \simeq \frac{c}{1000}$ 12 G (see Eq. 11), we obtain $DH_{KV} \simeq \frac{c}{1000}$ 4 G. A more accurate value of DH_{KV} could be obtained by making a series of experiments at a lower microwave frequency, e.g. 1.7 GHz as was done by Dahlberg[16]. Both of the above values of DH_{KV} are much smaller than the value of DH_{KV} obtained[16] for Er in Ag ($\frac{c}{1000}$ 20 G). This indicates that Er produces less distortions in Au than in Ag. The same conclusion can be drawn also from the residual linewidth extrapolated to zero concentration, which is 8 G for Er in Au (rolled samples, see Fig. 3) and 14.5 G for Er in Ag[16] (samples prepared by filing).

The residual linewidth extrapolated to zero concentration which we obtained for heated samples is approximately 4 G (see Fig. 3). This is the narrowest zero concentration residual linewidth ever reported for a localized impurity in a polycrystalline metal at X-band frequency.

A rough estimate of a lower and upper limit for the concentration of Er ions contributing to the resonance line after heating (for 1 hour) was calculated to be 25 and 50% of the value before heating respectively. Most of our experimental results are in good agreement with the value obtained as the lower limit. A comparison of the

linewidth in rolled samples with those obtained for filed samples in some of our experiments, as well as with values obtained for filed samples by other authors[23], shows that there is no appreciable difference in the linewidth of Er in Au in samples prepared by these two types of cold-working.

DH_o is the contribution to the residual linewidth due to random stresses. In our case the main source of the stresses are dislocations. The values of DH_o (for c=0) are 8 and 4 G for rolled and heated samples, respectively. The decrease in DH_o after heating demonstrates clearly a reduction in the stress around the Er impurities, which is consistent with a model of mobile dislocations and immobile impurities in the metal during heating[24]. We have assumed in our analysis of the linewidth that DH_o does not change with the concentration of Er. A more precise treatment should also take into account the effect of enhanced stabilization of dislocations by Er impurities[24]. We propose a model based on the segregation of Er ions to dislocations (subgrain boundaries) during heating, to explain the decrease in the linewidth and in the integrated intensity of the EPR line after heating. The simplest physically significant model[25] for subgrain boundary segregation predicts that the concentration at the subgrain boundary (c_b) is given by

$$c_b = \frac{c_m \exp(G_a/kT)}{(1 - c_m) + c_m \exp(G_a/kT)}$$

where c_m is the matrix solute concentration, G_a is the Gibbs free energy of binding to the subgrain boundary and kT has its usual

significance. If $c_m << 1$ and $G_a \lesssim kT$, then $c_b = c_m \exp(G_a/kT)$. The ratio c_b/c_m should according to this model, be independent of the initial concentration (doping level). From our results we have obtained $G_a \approx 0.1$ eV.

The process of segregation of impurities to dislocations causes a decrease in the linewidth due to two effects acting in parallel, one is a decrease in the number of Er ions contributing to the resonance line, and causing a decrease in the integrated intensity, the other is a decrease in the stress field.

The asymmetry parameter A/B was found to increase linearly with the concentration of Er (see Fig. 4). This concentration dependence of the A/B ratio is $2.0 + 0.6\text{x}10^{-3}c$ and $2.7 + 2.5\text{x}10^{-3}c$ in the rolled and heated samples, respectively. Several models were considered to explain this drastic increase in the A/B ratio after heating. At this stage we have no rigorous explanation for this behavior and more theoretical and probably also experimental work has to be performed.

We have examined the possibility of whether the changes in the features of the EPR line, caused by heating, might be due to oxidation, or clustering, or diffusion to the surface (causing a change in the concentration of Er in a surface layer), or changes in the valence state of Er^{3+}. Heating in air, hydrogen, and argon had approximately the same effect on the EPR line as heating in vacuum. This excludes the possibility of appreciable oxygen diffusion into the samples. This result is consistent with the

work of Svoboda[26] who has studied the internal oxidation of impurities in gold, and showed that heating in air or in a low pressure oxygen atmosphere results in extremely low solubility of oxygen in gold. It should be pointed out here that the solubility of Er in Au is very good. It was shown[27] that at 400C the solubility of Er in Au is about 0.5 at.%.

The recovery of all three characteristic features of the EPR line (ΔH, I, A/B) after polishing the heated samples also confirms our model of dislocation movement. Mechanical polishing introduces dislocations and causes dislocations to move through a metal. Thus dislocations can move away from the Er ions, and these Er ions,"freed from dislocations", can again contribute to the resonance line. Further, the polishing experiments also prove that heating of our samples (for 1 hour at 400C), did not cause either oxidation, or clustering, or diffusion, or valency changes of Er^{3+} in gold.

Additional support for our model was obtained from the successive rolling experiment. Linear recovery of the linewidth as function of percent of cold-work strongly suggests direct dependence of the linewidth on the production and movement of dislocations during cold-work.

The recovery of the linewidth and A/B ratio after etching indicates preferred segregation in a surface layer. We have not investigated the possible changes in the surface inpedance due to our treatments, however it seems quite acceptable that such changes might have an effect on the lineshape through a variation of the percent of

dispersion and absorption. Measurements of d.c. resistivity did not exhibit any appreciable changes between the rolled and heated samples, which also indicates that we are dealing with a surface effect.

A computer reconstruction of the resonance lines using a Lorentzian lineshape (see Figs. 8 to 11) and with the linewidth, A/B ratio, resonance field and intensity as fitted parameters, was in good agreement with the experimentally recorded EPR spectrum of rolled and heated samples as well. Stress fields cause inhomogeneous broadening of the resonance line, which should be reflected in a Gaussian lineshape. The good fit to a Lorentzian suggests that there are no dominant long range stress field effects due to dislocations in our samples and this is another supporting factor for our model proposing that the majority of the observed effects reported here are due to either stabilization of dislocations in the vicinity of Er ions, or movement of dislocations away from the Er ions.

The effects of cold-work on the conduction electron spin resonance linewidth in pure Al, Cu and Ag metals was investigated by Beuneu and Monod[28]. The research reported here is the first demonstration of the application of the EPR of magnetic impurities to the study of defects produced in metals by cold-working.

VI. SUMMARY AND CONCLUSIONS

We have shown in this work that the EPR technique can be used to study defects in metals. A detailed investigation of the features of the resonance lines of the dilute magnetic impurity Er^{3+} in Au,

in samples cold-worked (rolled and polished), heat treated in vacuum, air or hydrogen and ion bombarded (by argon and gold ions), provided information on the segregation of Er^{3+} ions to subgrain boundaries, on the local stress around the magnetic impurities and on the influence of the different treatments on the effective concentration of the magnetic impurities. Heating of the rolled samples reduced the EPR linewidth and intensity, and increased the value of the asymmetry parameter (the A/B ratio). Ion bombardment produced partial recovery, gradual deformation by successive rolling yielded almost complete recovery and mechanical polishing resulted in complete recovery of the linewidth, intensity and A/B ratio to values observed before heating. No appreciable variations were detected in the g-factor, hyperfine structure constant or the Korringa relaxation rate.

The extremely narrow absorption line of Er^{3+} obtained after the heat treatment is narrower than any other value reported previously for a magnetic impurity in polycrystalline metals at X-band, and thus makes it a sensitive probe for the study of defects in metals and alloys. A theoretical treatment is presented for the behavior of the linewidth. Theoretical estimates of the upper and lower limits of the number of Er ions contributing to the absorption line after the heat treatment are found to be in good agreement with the experimental results. Our results show that the EPR of magnetic impurities in metals is a promising technique for the study of interactions between magnetic impurities and defects produced in metals by cold working and ion bombardment. The extention of this work to other alloy systems, other treatments and other types of irradiation seems very challenging.

ACKNOWLEDGEMENT

This research was supported by a grant from the United States - Israel Binational Science Foundation (BSF), Jerusalem, Israel. The participation of Professor D.N. Seidman and Professor R. Orbach as cooperating investigators is gratefully acknowledged.

We wish to thank Professor D. Shaltiel and Professor V. Zevin for their interest and cooperation in this work and Mr. A. Grayevskey for his invaluable help in sample preparation.

REFERENCES

1. "Defects and Radiation Damage in Metals", M.W. Thomson, Cambridge, 1969; "Lattice Defects and their Interactions", R.R. Hasiguti, Gordon and Breach, 1967.

2. A comprehensive review of the experimental results of EPR of magnetic impurities in metals has been recently published: "Electron Spin Resonance of Magnetic Ions in Metals. An Experimental Review", R.H. Taylor, Advances in Physics 24, 681 (1975).

3. "Electron Paramagnetic Resonance Studies of Irradiation Effects in Dilute Magnetic Alloys", J.T. Suss, Comprehensive Report, Grant No. 777, Submitted to the BSF., Dec. 1977.

4. "Paramagnetic resonance of S-state ions in metals", M. Peter, D. Shaltiel, J.H. Wernick, H.J. Williams, J.B. Mock and R.C. Sherwood, Phys. Rev. 126, 1395 (1962).

5. "Electron spin resonance absorption in metals. I. Experimental". G. Feher and A.F. Kip, Phys. Rev. 98, 337 (1955); "Electron spin resonance absorption in metals. II. Theory of electron diffusion and the skin effect", F.J. Dyson, Phys. Rev. 98, 349 (1955).

6. See e.g. "Electron Spin Resonance, A Comprehensive Treatise on Experimental Techniques", C.P. Poole, Jr., Interscience Publishers, 1967, Chap. 14 and 20.

7. "Reference Data for Radio Engineers". 4th Edition International Telephone and Telegraph Corp., N.Y., 1956.

8. "Skew scattering by rare-earth impurities in silver, gold and aluminum", A. Fert and A. Friederich, Phys. Rev. B 13, 397 (1976).

9. "Effects of Impurities on Recovery Stages in Electron-Irradiated Gold", K. Nakata, K. Ikeuchi, H. Hirano, K. Furukawa and J. Takamura, Proc. Int. Conf. on Fundamental Aspects of Radiation Damage in Metals, Gatlinburg, Tennessee, Oct. 6-10, 1975, M.T. Robinson and F.W. Joung,Jr., Editors, Vol. 1, p.622.

10. "Exchange and hyperfine interaction in Ag:Mn dilute alloys", D. Davidov, C. Rettori, R. Orbach, A. Dixon and E.P. Chock, Phys. Rev. B 11, 3546 (1975).

11. "Dynamics of Dilute Magnetic Alloys and Nonequilibrium Superconductivity", E.D. Dahlberg, Ph.D. Thesis, University of California, Los Angeles, California, U.S.A., 1978 (unpublished).

12. This chapter is based on a presently unpublished report written by Prof. V. Zevin of the Hebrew University, Jerusalem.

13. "Dynamical Properties of s-d Interactions", H. Hasegawa, Progr. Theoretical Physics 21, 483 (1959).

14. "Transmission Spin Resonance of Coupled Local-Moment and Conduction-Electron Systems", S. Schultz, M. Schanaberger and P.M. Platzman, Phys. Rev Lett. 19, 749 (1967).

15. "Effect of exchange with local moments and hyperfine interaction on the electron-spin-resonance line shapes in metals", J.H. Pifer and R.T. Longo, Phys. Rev. B 4, 3797 (1971).

16. "Investigation of the residual linewidth of Ag:Er dilute alloys", E.D. Dahlberg, Phys. Rev. B 16, 170 (1977).

17. "Theory of nuclear resonance intensity in dilute alloys", W. Kohn and S.H. Vosko, Phys. Rev. 119, 912 (1960).

18. "Electron Spin Resonance of Gd in the Intermetallic Compounds, YCu, YAg and LaAg: Wave Vector Dependence of the Exchange Interaction", D. Davidov, K. Maki, R. Orbach, C. Rettori and E.P. Chock, Solid State Commun. 12, 621 (1973).

19. "Hyperfine splitting of Er and Yb resonances in Au: A separation between the atomic and covalent contribution to the exchange integral", L.T. Tao, D. Davidov, R. Orbach and E.P. Chock, Phys. Rev. B 4, 5 (1971).

20. "Dipolar Broadening of Magnetic Resonance Lines in Magnetically Dilute Crystals", C. Kittel and E. Abrahams, Phys. Rev. 90, 238 (1953).

21. "Copper Nuclear Resonance Line in Cu Mn Alloys" , R.E. Behringer, J. Phys. Chem. Solids 2, 209 (1957).

22. "Dynamic Nuclear Orientation", C.D. Jeffries, Interscience, N.Y. 1963.

23. "Crystalline-Field Effects in the EPR of Er in Various Cubic Metals", C. Rettori, D. Davidov and H.M. Kim, Phys. Rev. B 8, 5335 (1973).

24. "Dislocations", J. Friedel, Pergamon Press, London, 1964, Chapter XIII.

25. "Grain Boundaries in Metals", D. McLean, Clarendon Press, Oxford, 1956, Chapter V;
"Thermodynamics of Solids", R.A. Swalin, John Wiley and Sons, 2nd Edition, 1972, pp.285-288.

26. "Internal oxidation of impurities in gold", P. Svoboda, J. Phys. F: Metal Phys. 8, 1757 (1978).

27. "Gold-Rich Rare-Earth-Gold Solid Solutions", P.E. Rider, K.A. Gschneidner, Jr., and O.D. McMasters, Trans. Metallurg. Soc. of AIME, 233, 1488 (1965).

28. "Conduction-electron spin resonance in cold-worked Al, Cu and Ag: The spin-flip cross section of dislocations", F. Beuneu and P. Monod, Phys. Rev. B 13, 3424 (1976).

T A B L E I

Increase in the intensity I of the resonance line and Er concentration c (concentration of the Er ions contributing to the resonance line) as a function of cold-working in a Au sample doped with 1000 ppm Er. The intensity of the 0.75mm thick rolled sample was taken as 1.

	rolled	heated	heated sample successively rolled at room temperature		
Sample thickness d(mm)	0.75	0.75	0.53	0.25	0.15
$\Delta h/h_o$	-	0	0.29	0.67	0.8
$I^{(a)}$	1	0.05	0.05	0.17	0.37
$c^{(b)}$ (ppm)	1000	130	130	310	515

(a) I was calculated as $(A+B)(\Delta H)^2$ Corrections were made for spectrometer gain and sensitivity.

(b) In the estimation of the concentration c of the Er ions contributing to the resonance line, compensation was also made for the changes in the skin depth due to the change in effective concentration. (If c_1 and c_2 are the concentrations before and after a treatment respectively, and N_1 and N_2 are the number of spins in the skin depth before and after the treatment respectively, we obtain $c_2 = (N_2/N_1)^{2/3} c_1$. Since $N \propto c\,\delta \propto c(c)^{\frac{1}{2}} = c^{3/2}$).

T A B L E I I

Results of ion implantation into heated samples of Au doped with 1500 ppm Er. Samples were kept at 77K during implantation.

	rolled	heated	after implanting 2.5×10^{16} Ar ions/cm^2
ΔH (Gauss)	28.6	13.4	20.9
A/B	2.62	6.4	4.2
Intensity I[(a)]	1	0.14	0.26
Er concentration c[(b)] (ppm)	1500	400	600

	rolled	heated	after implanting 2×10^{16} Au ions/cm^2
H (Gauss)	31.0	12.3	17.7
A/B	2.58	6.56	4.7
Intensity I[(a)]	1	0.1	0.2
Er concentration c[(b)] (ppm)	1500	320	510

For notes (a) and (b) see Table I.

T A B L E I I I

Computer fitted EPR parameters of a rolled and heated sample of Au doped with 1500 ppm Er.

	rolled	heated
ΔH (Gauss)	(37.31 $\pm$ 0.30)	(18.68 $\pm$ 0.20)
Dispersion	(50.3 $\pm$ 0.7)%, (A/B $\simeq$ 2.6)	(82.8 $\pm$ 1.4)%, (A/B $\simeq$ 5.7)
H_o	(994.19 $\pm$ 0.28) Gauss	(992.68 $\pm$ 0.20) Gauss
$I_o^{(c)}$	2.05 $\pm$ 0.01	1.91 $\pm$ 0.03

(c) I_o is a multiplication factor in arbitrary units, used to adjust the intensity of the computed line to that of the measured one.

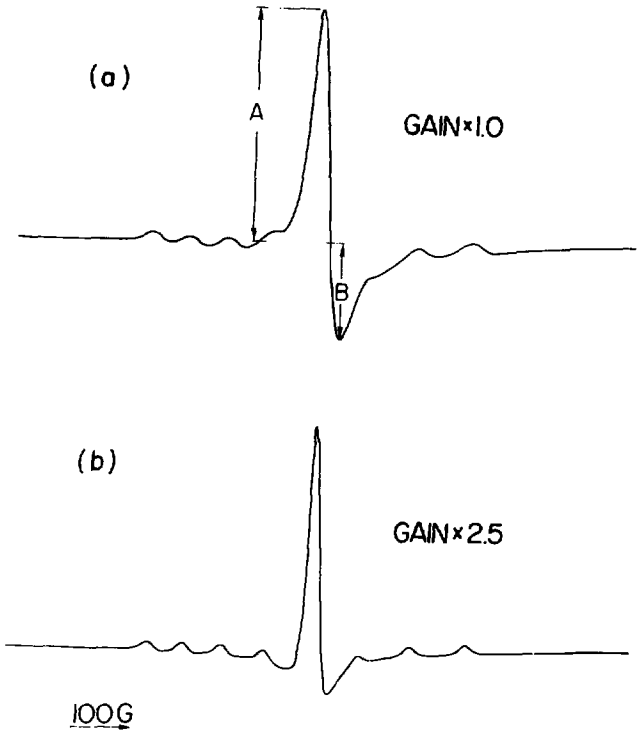

Figure 1

The EPR spectrum of Er in Au. Doping level = 1000 ppm, f = 9.4 GHz, T = 1.65K.

a - Rolled sample. A and B, the maximum and minimum of the first derivative of the absorption line, define the asymmetry parameter called the A/B ratio.

b - Same sample after heating for 1 hour at 400 C in a vacuum of 10^{-6} torr.

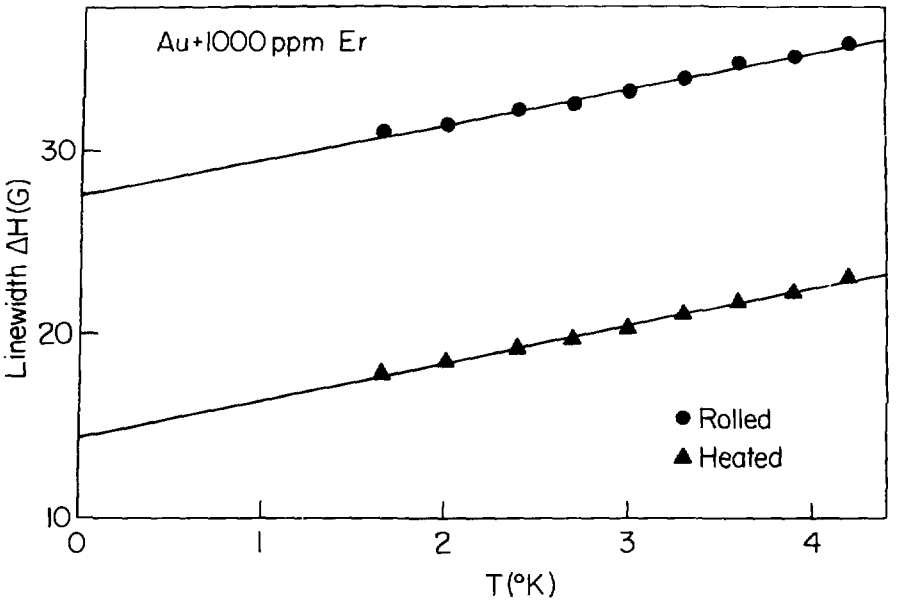

Figure 2

The EPR linewidths ΔH of a rolled and a heated (for 1 hour at 400C in a vacuum of 10^{-6} torr) sample of Au doped with 1000 ppm Er, as a function of temperature, f = 9.4GHz. The linewidths for each measured point were determined according to a procedure outlined in Ref. 4. The solid lines are least square best fits to the experimental points.

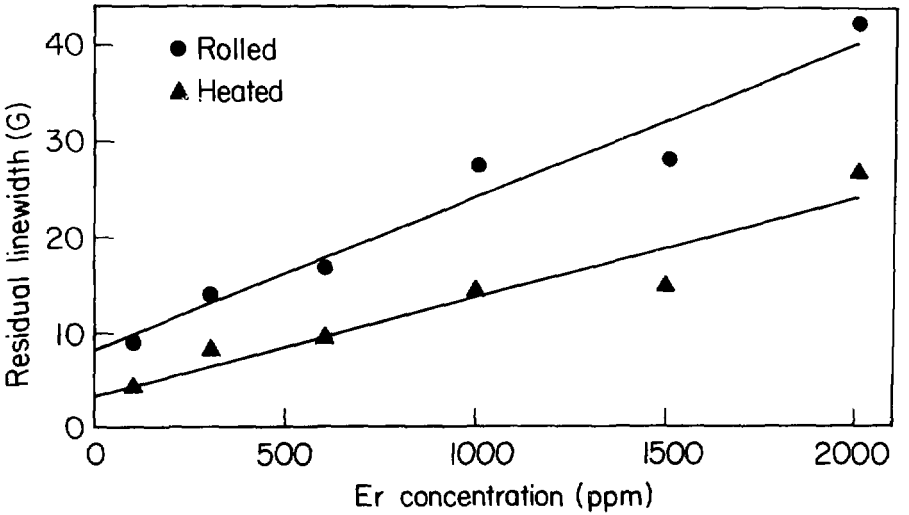

Figure 3

The residual linewidth in rolled and heated samples of Au doped with Er as a function of Er concentration (doping level). The circles designate the sample measured after rolling, and the triangles represent the same sample after heating for one hour at 400C in a quartz tube under a vacuum of 10^{-6} torr.

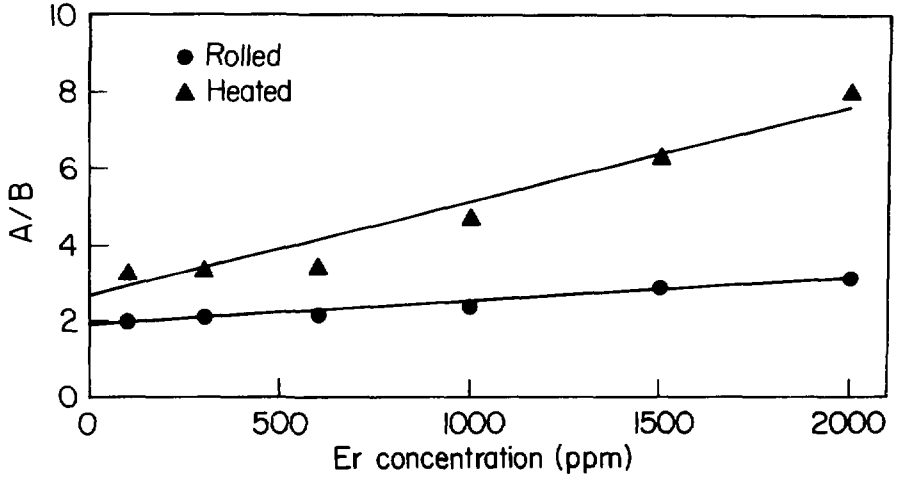

Figure 4

The A/B ratio as a function of the concentration (doping level) of Er in Au, in rolled and heated samples. Heating conditions same as in Fig. 3.

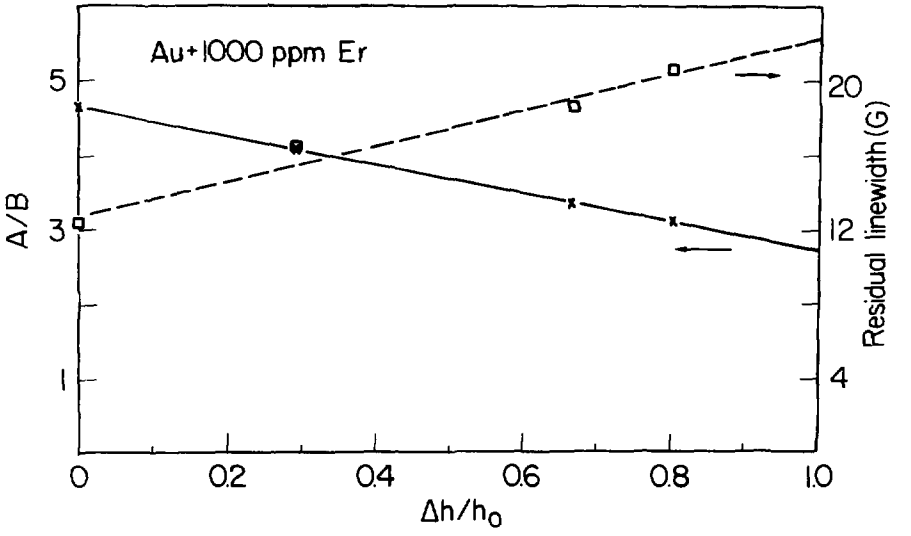

Figure 5

Residual linewidths (□) and A/B ratios (x) as a function of cold-work $\Delta h/h_o$, in a sample of Au doped with 1000 ppm Er. $\Delta h = h_o - h_i$; h_o=0.75mm is the thickness of the heated sample, and h_i is the thickness of the sample after the i-th rolling step. The solid line and the broken line are least square best fits to the data points.

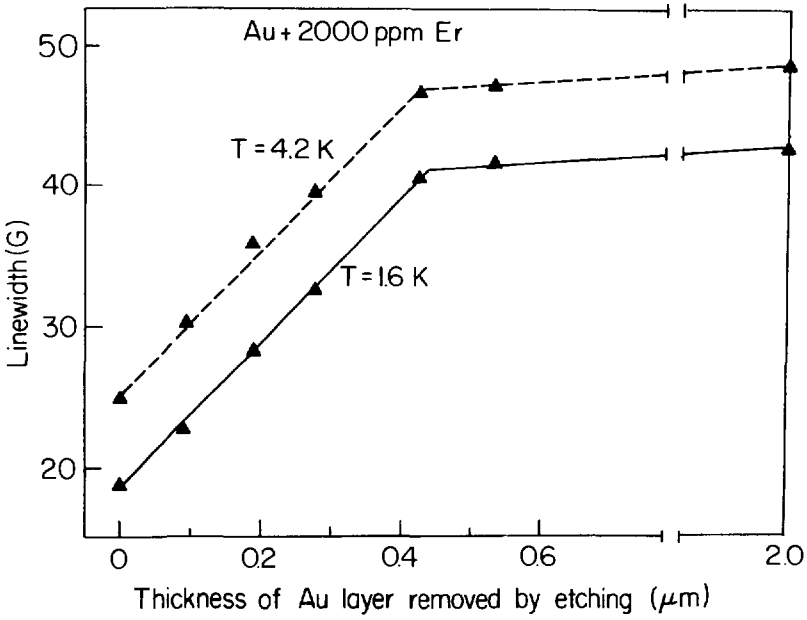

Figure 6

EPR linewidth in a heated sample of Au doped with 2000 ppm Er as a function of the thickness of a surface layer removed by successive etching. The solid and broken lines serve as a guide to the eye for experimental points obtained at 1.65K and 4.2K respectively.

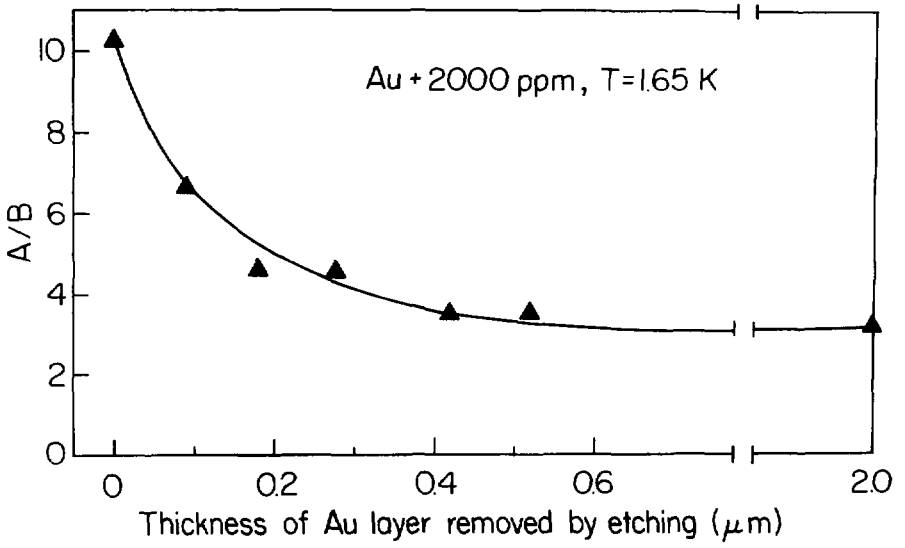

Figure 7

The A/B ratios in a heated sample of Au doped with 2000 ppm Er as a function of the thickness of a surface layer removed by successive etching. The line serves as guide to the eye only. The experimental points, designated by triangles, are taken from the same measured spectra as those for the 1.65K curve in Fig. 6.

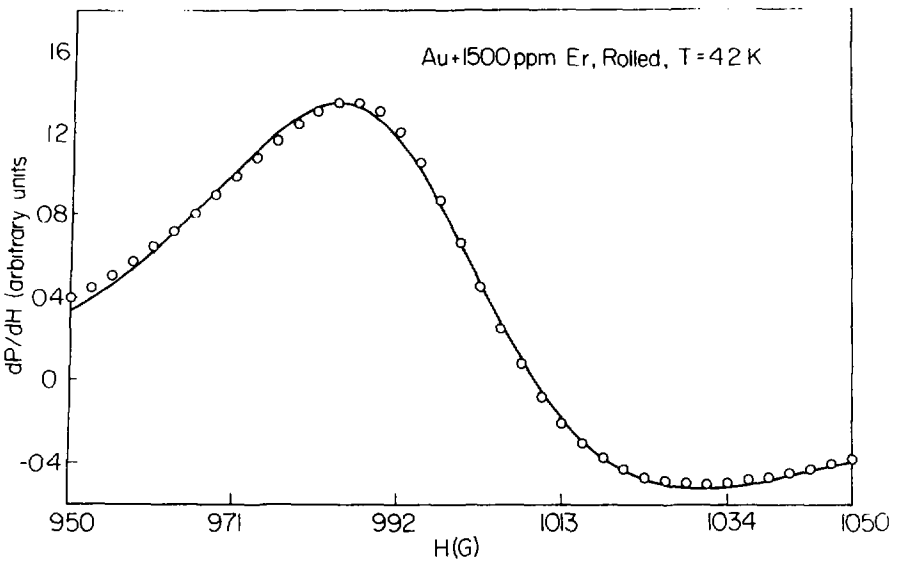

Figure 8

Computer fitted first derivative of the central absorption line of 1500 ppm Er in Au in a rolled sample. The experimental points were extracted from a recording taken at a frequency of 9.4 GHz and T=4.2K, with the external magnetic field swept over a range of 100G. The solid line is the computer fit over a range of 100G using a Lorentian lineshape with the following fitted parameters: linewidth ΔH, the percentage of admixture of dispersion and absorption (determining the A/B ratio), the resonance field H_o and the intensity. The fit also includes the contribution of the hyperfine structure. The fitted parameters are given in Table III.

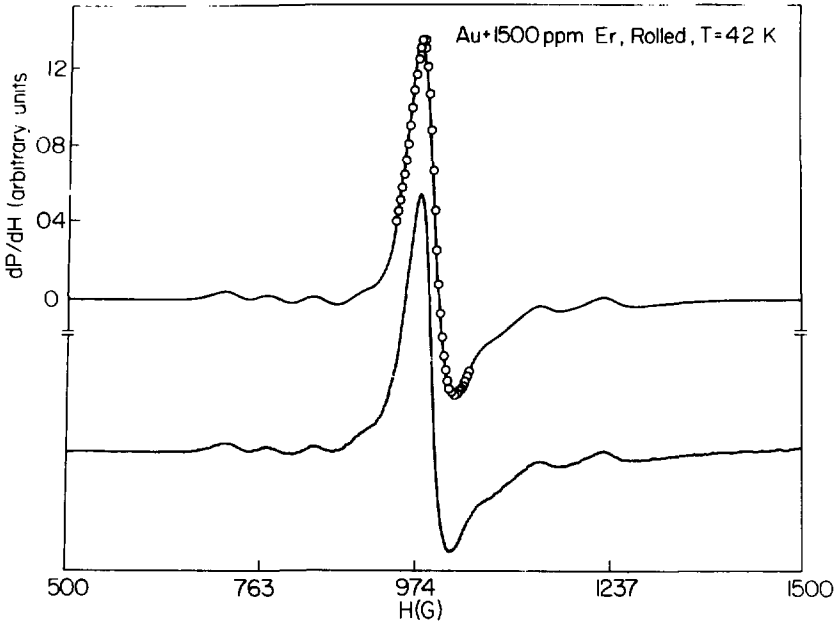

Figure 9

The upper curve is a computer calculated EPR spectrum of 1500 ppm Er in Au in a rolled sample, over a range of 1000G, including the same experimental points (designated here also by circles) and using the same fitted parameters and lineshape as in Fig. 8. The lower curve is a trace of an experimental spectrum, taken with the same sample and under the same conditions as described in Fig. 8, except that the external magnetic field is swept over a range of 1000G.

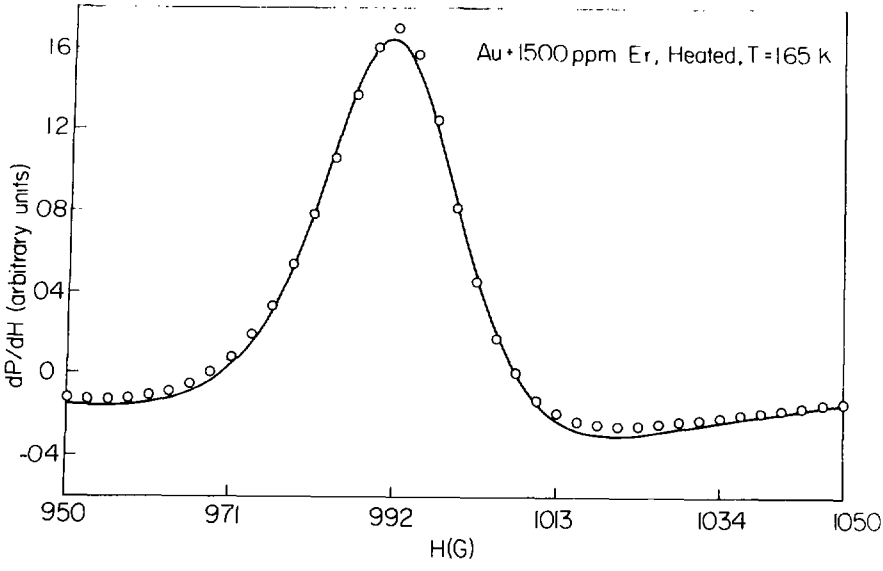

Figure 10

Computer fitted first derivative of the central absorption line of 1500 ppm Er in Au in a heated sample (the spectrum of the same sample rolled is shown in Figs. 8 and 9). The experimental points were e tacted from a recording taken at a frequency of 9.4 GHz at T=1.65K, with the external magnetic field swept over a range of 100G. The solid line is the computer fit using a Lorentzian lineshape with sweep and fitting parameters as described in Fig. 8. Here also the fit includes the contribution of the hyperfine structure. The fitted parameters are given in Table III.

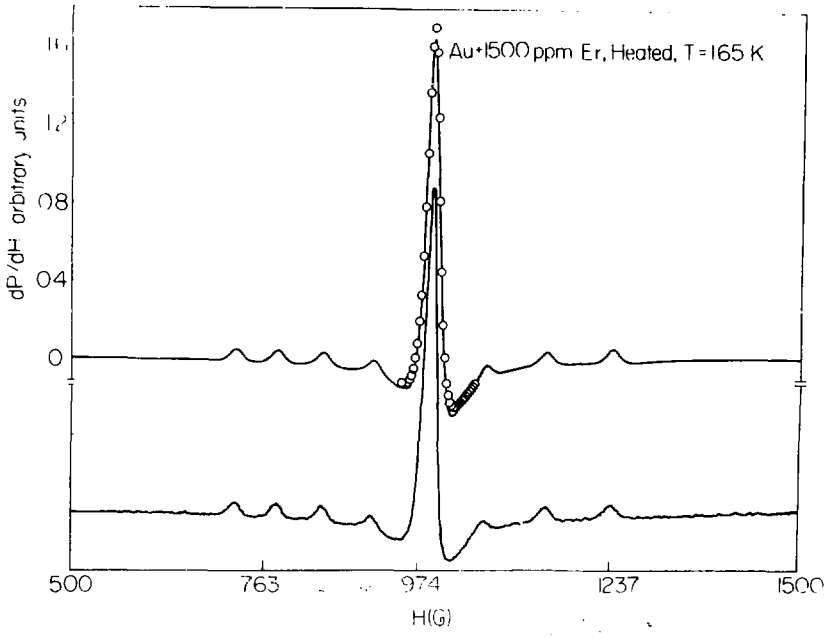

Figure 11

The upper curve is a computer calculated EPR spectrum in a heated sample of Au doped with 1500 ppm Er, over a range of 1000 G, using the same experimental points as in Fig. 10 (designated here also by circles) and the same fitted parameters and lineshape. The lower curve is a trace of an experimental spectrum taken with the same sample and under the same conditions as described in Fig. 10, except that the external magnetic field is swept over a range of 1000 G.

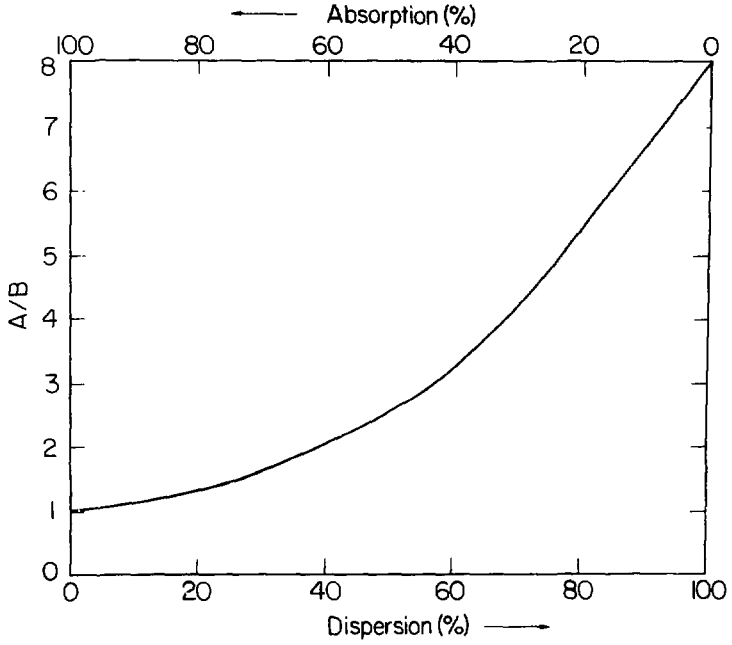

Figure 12

The A/B ratio as a function of the percent absorption and dispersion calculated for a Lorentzian lineshape (without the hyperfine structure). Percent absorption + percent dispersion = 100%.

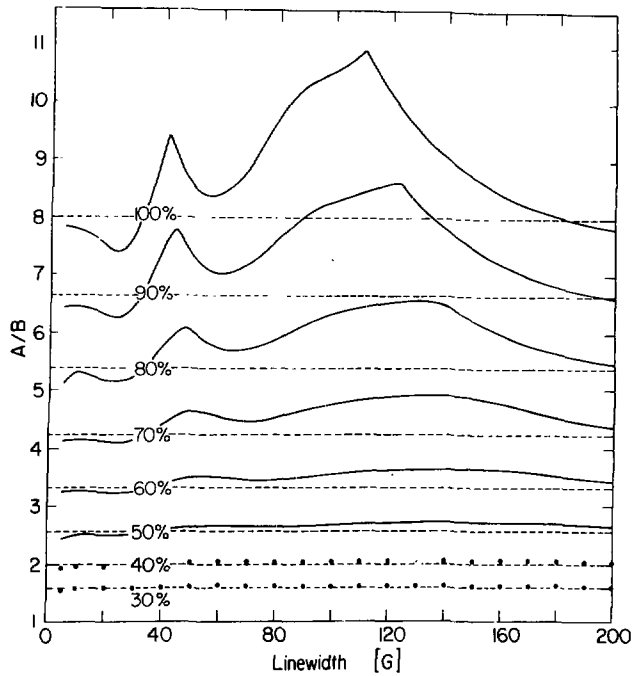

Figure 13

Calculated variations in the A/B ratio due to the hyperfine structure, as a function of the linewidth for the case of Er with a Lorentzian lineshape. The existence of the hyperfine structure in addition to a strong central line (due to the even isotope), causes a change in the lineshape of the central line and consequently an apparent A/B ratio, which deviates from the actual A/B ratio. The full lines represent the deviations from the actual A/B ratio (represented by the broken line) due to the superposition of the hyperfine structure, for 8 different cases of admixture of dispersion and absorption between 30% and 100% dispersion. For 50% dispersion or less ($A/B \simeq 2.5$) the discrepancy is negligible. For the 30% and 40% cases full circles are drawn instead of the solid lines.

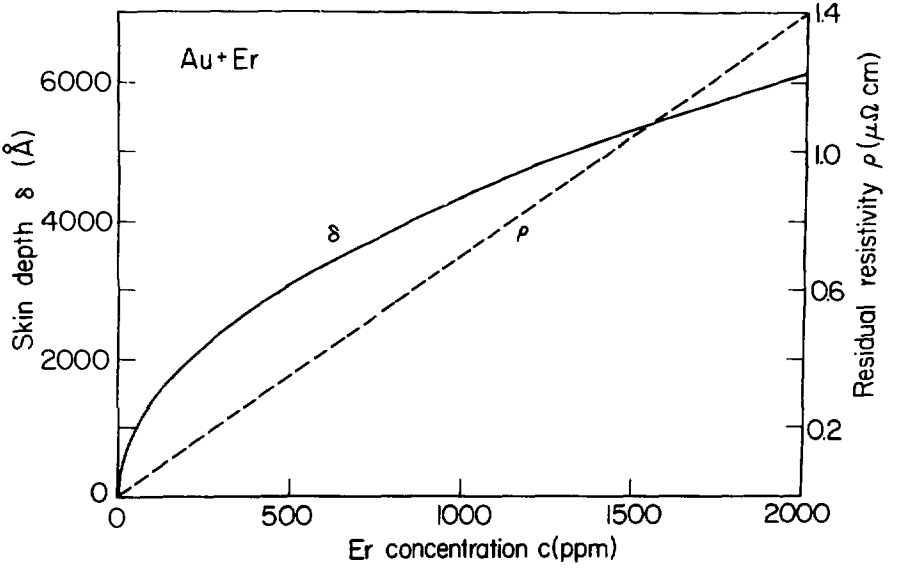

Figure 14

Skin depth δ and residual resistivity ρ in Au doped with Er, as a function of the concentration of Er, using ρ = 7μΩcm per at.% of Er as given in Ref. 8, and a frequency of 9.4 GHz for δ. In this graph, the contribution of the residual resistivity of pure Au, being very small as compared to the contribution due to Er ($\rho_{Au(pure)} \simeq 1.2$ nΩcm, see e.g. Ref. 9), was neglected.

PUBLICATIONS

1. "An EPR study of defects in dilute Au:Er alloys"
A. Raizman, J.T. Suss, D.N. Seidman, D. Shaltiel, V. Zevin, and R. Orbach,
Bull. Israel Phys. Soc., 25, 43 (1979)
Paper presented at the Annual Meeting of the Israel Physical Society,
Beer-Sheva, April 1-2, 1979.

2. "EPR study of cold-worked dilute gold-erbium alloys"
A. Raizman, J.T. Suss, D.N. Seidman, D. Shaltiel, V. Zevin and R. Orbach
J. Appl. Phys. 50, 7735 (1979).